Int. J. Solids Structures, 1973, Vol. 9, pp. 115 to 127. Pergamon Press. Printed in Great Britain

INITIAL POSTBUCKLING BEHAVIOR OF OPTIMALLY DESIGNED COLUMNS AND PLATES

JAMES C. FRAUENTHAL

Anderson Hall, Tufts University, Medford, Massachusetts 02155

Abstract—The initial postbuckling behavior of optimally designed structures of two generic types is investigated. The structures are straight, simply-supported, inextensional columns, loaded by axial thrust and flat, simply-supported, axisymmetric circular plates, loaded by radial thrust. The structures are optimal in the sense that they withstand the largest possible loads prior to buckling, while satisfying fixed volume and minimum allowable gage constraints. The stability analysis is based upon Koiter's general theory of the postbuckling behavior of structures.

INTRODUCTION

PROVIDING additional stiffness to structures by means of reinforcements may not gain as much strength as is indicated by the classical buckling calculation. This can happen because the stiffening can increase the sensitivity of the structures to small geometric imperfections [1]. This tendency can be observed for a large variety of structures. A striking example of this type of behavior is found if one reinforces circular cylindrical shells with either inside or outside stiffeners [2].

In this paper the initial postbuckling behavior of optimally designed structures of two generic types is investigated. The structures are straight, simply-supported columns, loaded by axial thrust and flat, simply-supported, axisymmetric circular plates, loaded by radial thrust. In optimally designing these structures the classical buckling loads are maximized, subject to the restrictions that the volume of structural material and minimum allowable gage are specified.

Before proceeding, one important point should be noted. Masur [3] has demonstrated that all of the structures investigated in this paper necessarily exhibit stable initial postbuckling behavior. (This proof for columns is repeated later in this paper.) The purpose of this paper is to determine how the initial postbuckling stiffness of the structures examined is effected by optimization.

The postbuckling analysis is based upon Koiter's general theory [4] as restated by Budiansky [5, 6]. Since the optimal design techniques and results have already been presented by the author [7, 8] and the postbuckling analysis procedure is well accepted, no effort is made to fill in details in the remainder of this paper.

INEXTENSIONAL COLUMNS

Buckling and initial postbuckling equations

In this section, the governing equations for the buckling and initial postbuckling of a straight, inextensional, simply-supported, variable gage column under axial thrust are

given. The details of the derivation are based upon the general formulation given by Budiansky [5]. The question of the optimal design against buckling (the actual gage variation along a column) is deferred until the next section.

The variational statement of equilibrium for an inextensional column of length L under compressive axial load P is given by

$$\int_0^L M\delta\kappa \, dx = P\int_0^L \delta\left(\frac{d\Delta}{dx}\right) dx \tag{1}$$

where M is the bending moment, κ the curvature, Δ the end-shortening and the geometry is shown in Fig. 1. The quantities M, κ and $(d\Delta/dx)$ are defined by the relations

$$M = EI\kappa \tag{2}$$

$$\kappa = \frac{d^2y/dx^2}{[1-(dy/dx)^2]^{\frac{3}{2}}} \tag{3}$$

$$\left(\frac{d\Delta}{dx}\right) = [1-(dy/dx)^2]^{\frac{1}{2}} - 1 \tag{4}$$

where EI is the bending stiffness.

It is convenient for our purposes to define the moment of inertia $I(x)$ in terms of the cross-sectional area of structural material $A(x)$. The columns considered have

$$I(x) = kLV\left[\frac{LA(x)}{V}\right]^n \tag{5}$$

where k and n are adjustable positive constants and V is the volume of structural material, which is related to $A(x)$ by

$$\int_0^L A(x)\, dx = V. \tag{6}$$

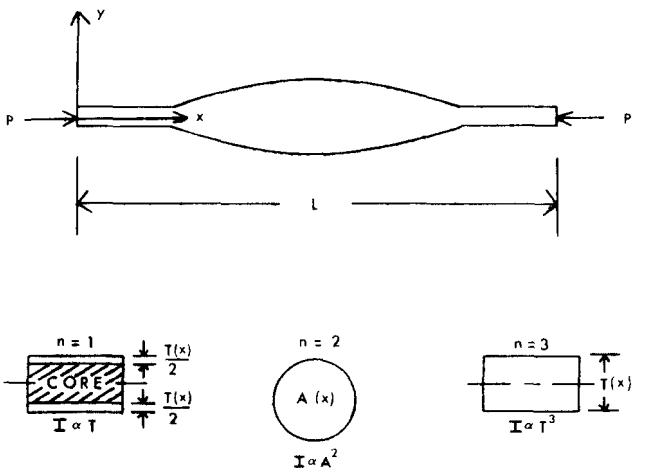

FIG. 1. Column geometry, displacements and loading.

Along with appropriate choices of k, $n = 1$, 2 and 3 model, respectively, sandwich cross-sections with fixed width and depth light cores and variable depth cover sheets, solid cross-sections of variable size but fixed shape, and solid rectangular cross-sections of fixed width and variable depth (see Fig. 1). The reason for including (5) and (6) will become apparent in the section on optimization.

Combining equations (1)–(5) in non-dimensional form and anticipating that all columns of interest are symmetrical about their mid-points, $x = L/2$, leads to

$$\int_0^{\frac{1}{2}} \{\tau^n[(1+\eta^2)\eta'\delta\eta' + \eta(\eta')^2\delta\eta] - \lambda(n+\tfrac{1}{2}\eta^3)\delta\eta\}\, \mathrm{d}\xi = 0 \tag{7}$$

where

$$\lambda = \frac{PL}{kEV}, \qquad \tau = \frac{AL}{V}, \qquad \eta = \frac{\mathrm{d}y}{\mathrm{d}x}, \qquad \xi = \frac{x}{L} \quad \text{and} \quad (\,)' = \frac{\mathrm{d}}{\mathrm{d}\xi}(\,).$$

Note that in arriving at this expression, the binomial expansion has been used and only terms whose order causes them to effect the initial postbuckling have been retained.

In order to investigate the buckling and initial postbuckling behavior an asymptotic perturbation expansion of the solution valid near the bifurcation point is sought in the form

$$\lambda = \lambda_c[1 + a\varepsilon + b\varepsilon^2 + \ldots] \tag{8}$$

$$\eta = \varepsilon\eta_1 + \varepsilon^2\eta_2 + \varepsilon^3\eta_3 + \ldots \tag{9}$$

where λ_c is the classical, non-dimensional buckling load of the perfect column, η_1 is the classical buckling mode and ε is a scalar parameter whose meaning will be identified shortly.

Substitution of (8) and (9) into (7), along with simple-support boundary conditions, leads to the classical buckling problem

$$[\tau^n\eta_1']' + \lambda_c\eta_1 = 0, \qquad \tau^n\eta_1' = 0 \quad \text{at} \quad \xi = 0, \qquad \eta_1 = 0 \quad \text{at} \quad \xi = \tfrac{1}{2}. \tag{10}$$

It is necessary at this point to normalize η_1. It is convenient to choose

$$\int_0^{\frac{1}{2}} \dot{\eta}_1\, \mathrm{d}\xi = 1. \tag{11}$$

This choice fixes the value of the buckling deflection at the midpoint of the column, hence the scalar parameter ε can now be identified as a measure of the contribution of the buckling mode η_1 to the buckled state.

If the higher order terms in the asymptotic expansion of η are required to be orthogonal to η_1 by the relationship

$$\int_0^{\frac{1}{2}} \eta_1\eta_j\, \mathrm{d}\xi = 0 \quad \text{for} \quad j = 2, 3, \ldots \tag{12}$$

then (7)–(9) lead to the three expressions

$$\lambda_c = \frac{\int_0^{\frac{1}{2}} \tau^n (\eta_1')^2 \, d\xi}{\int_0^{\frac{1}{2}} \eta_1^2 \, d\xi} \tag{13}$$

$$a = 0 \tag{14}$$

$$b = \frac{(2/\lambda_c)\int_0^{\frac{1}{2}} \tau^n \eta_1^2 (\eta_1')^2 \, d\xi - \frac{1}{2}\int_0^{\frac{1}{2}} \eta_1^4 \, d\xi}{\int_0^{\frac{1}{2}} \eta_1^2 \, d\xi}. \tag{15}$$

Equation (13) has been included as it is used in the derivation of the optimization equations. Equations (14) and (15) serve to describe the behavior of λ in the initial postbuckling regime. Since the nondimensional load λ is an even function of the buckling amplitude ε, $a = 0$ and the initial postbuckling behavior depends upon the sign and magnitude of b. It can be seen from (8) that if the sign of b is negative the load carrying capacity of a column decreases after buckling, while if b is positive it increases. In the terminology of [5], with $a = 0$, $b < 0$ corresponds with imperfection sensitivity and $b > 0$ with imperfection insensitivity.

It will now be proved that $b > 0$ regardless of the actual shape $\tau(\xi)$ of a column. If (10) is solved for η_1, and this quantity substituted into the second integral in (15), one integration by parts, and the boundary conditions from (10) lead to

$$b = \frac{\int_0^{\frac{1}{2}} \tau^n \eta_1^2 (\eta_1')^2 \, d\xi}{2\lambda_c \int_0^{\frac{1}{2}} \eta_1^2 \, d\xi}. \tag{16}$$

Since the column gage is non-negative, $\tau(\xi) \geq 0$ over the entire column. Also since $\lambda_c \geq 0$ it is readily seen from the form of (16) that $b > 0$. Hence all of the columns to be investigated are insensitive to initial imperfections in the sense of [5]. That is, small imperfections do not result in a large reduction of the buckling load.

It can be seen from (16) that the magnitude of b depends upon the normalization of the buckling mode. It is preferable to use a measure of the postbuckling stability which is independent of the normalization. Therefore, the value of the slope H of the loading versus end-deflection curve immediately after bifurcation is used instead of b. Comparison of (4), (8) and (9) leads to the desired result:

$$\left(\frac{\lambda}{\lambda_c}\right) = 1 + H\left(\frac{\Delta}{L}\right) + \ldots$$
$$H \equiv \frac{b}{\int_0^{\frac{1}{2}} \eta_1^2 \, d\xi} \tag{17}$$

where the fact that $a = 0$ has been used. The significance of H is illustrated in the insert in Fig. 2. [Note that the intercept of this curve is at $(\lambda/\lambda_c) = 1$ because the columns have been assumed inextensional.] It is apparent that the larger the value of H, the greater the initial postbuckling stiffness.

Constrained optimal design equations and solution

Optimization amounts to choosing the non-dimensional cross-sectional area distribution $\tau(\xi)$ so as to maximize the classical buckling load λ_c [as given by (13)] subject to

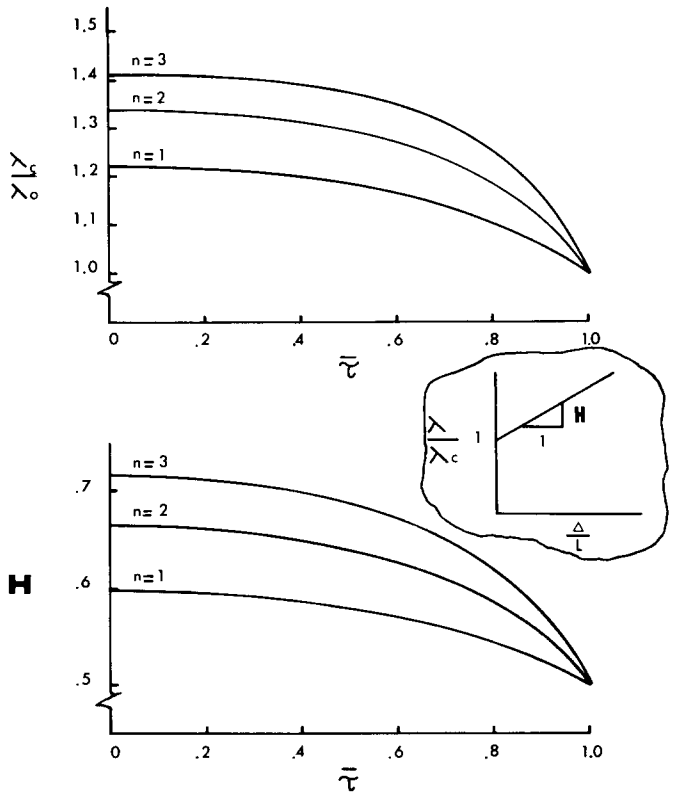

FIG. 2. Buckling and initial postbuckling behavior of columns.

the restriction that the volume of structural material is specified, thus

$$\int_0^{\frac{1}{2}} \tau \, d\xi = \tfrac{1}{2}. \tag{18}$$

This expression is simply equation (6) written for one-half of the column, in terms of the non-dimensional variables. The problem stated thus far is referred to as one of unconstrained optimization. For simple-support boundary conditions, solutions for $n = 1$, 2 and 3 are well known [9–11]. In all cases, τ goes to zero and consequently the stress to infinity at the simply-supported column ends. To prevent infinite prebuckling stresses from occurring the constraint is imposed that the cross-sectional area of the column may nowhere be less than some specified value $\bar{A}$. In non-dimensional form this is equivalent to demanding that

$$\tau \geq \bar{\tau} \tag{19}$$

where

$$\bar{\tau} = \frac{LA}{V}.$$

The remainder of the formulation of this problem is omitted, because an equivalent problem is treated in detail in [7]. There, a constraint is placed upon the maximum allowable prebuckling stress instead of the minimum allowable gage. It is, however, proven there that these two problems are identical for columns. The nature of the constrained optimal solution is now briefly described.

A solution is sought in the region $0 \leq \xi \leq \frac{1}{2}$ which maximizes the classical buckling load λ_c, and satisfies both (18) and (19). It is found that two types of regions occur. In the region $0 \leq \xi \leq \xi_0$, the constraint is active, thus $\tau = \bar{\tau}$ and in $\xi_0 \leq \xi \leq \frac{1}{2}$, the constraint is inactive, so $\tau > \bar{\tau}$. The value of the transition point, ξ_0, cannot be determined *a priori*, but rather is part of the solution. It is also found that at the transition point ξ_0, τ, η_1 and η_1' are all continuous, though in general τ' is discontinuous.

Families of optimal solutions, parameterized by $\bar{\tau}$ and n can be found analytically. These solutions are now listed. In the constrained region, $0 \leq \xi \leq \xi_0$:

$$\eta_1 = \left[\frac{(n+1)\lambda_c}{\hat{\tau}^{n+1}}(\hat{\tau}-\bar{\tau})\right]^{\frac{1}{2}} \frac{\cos[(\lambda_c/\bar{\tau}^n)^{\frac{1}{2}}\xi]}{\cos[(\lambda_c/\bar{\tau}^n)^{\frac{1}{2}}\xi_0]} \tag{20}$$

$$\tau = \bar{\tau} \tag{21}$$

where $\hat{\tau}$ is the value of τ at $\xi = \frac{1}{2}$. In the unconstrained region, $\xi_0 \leq \xi \leq \frac{1}{2}$:

$$\eta_1 = \left[\frac{(n+1)\lambda_c}{\hat{\tau}^{n+1}}(\hat{\tau}-\tau)\right]^{\frac{1}{2}} \tag{22}$$

$$\xi = \frac{1}{2}\left[1 - \left(\frac{n+1}{\lambda_c}\right)^{\frac{1}{2}} \int_{\tau}^{\hat{\tau}} \frac{t^{[(n-1)/2]}\,dt}{(\hat{\tau}-t)^{\frac{1}{2}}}\right]. \tag{23}$$

It is noted that the integral in (23) is easily performed for integer n. For specified values of n and $\bar{\tau}$, the solution is completed by simultaneously solving the following three equations for λ_c, ξ_0 and $\hat{\tau}$.

$$\tan\left[\left(\frac{\lambda_c}{\bar{\tau}^n}\right)^{\frac{1}{2}}\xi_0\right] = \left[\frac{\bar{\tau}}{(n+1)(\hat{\tau}-\bar{\tau})}\right]^{\frac{1}{2}} \tag{24a}$$

$$\xi_0 = \frac{1}{2} - \frac{[(n+2)/2](1-\bar{\tau}) - \{[(n+1)/\lambda_c]\bar{\tau}^{n+1}(\hat{\tau}-\bar{\tau})\}^{\frac{1}{2}}}{[(n+1)\hat{\tau}-(n+2)\bar{\tau}]} \tag{24b}$$

$$\xi_0 = \frac{1}{2}\left[1 - \left(\frac{n+1}{\lambda_c}\right)^{\frac{1}{2}} \int_{\bar{\tau}}^{\hat{\tau}} \frac{\tau^{[(n-1)/2]}\,d\tau}{(\hat{\tau}-\tau)^{\frac{1}{2}}}\right]. \tag{24c}$$

Values of λ_c, ξ_0 and $\hat{\tau}$ can be extracted from (24) for two limiting cases. If $\bar{\tau} = 1$, then for all n, $\hat{\tau} = 1$, $\xi_0 = \frac{1}{2}$ and $\lambda_c \equiv \lambda_0 = \pi^2$. These values describe the solution for the prismatic column; the one for which $\tau = 1$ along the entire length. If $\bar{\tau} = 0$, then the solutions reproduce those for unconstrained optimal design, with $\hat{\tau} = (n+2)/(n+1)$, $\xi_0 = 0$ and

$$\lambda_c = \pi \frac{(n+2)^n}{(n+1)^{n-1}}\left\{\frac{\Gamma[(n+1)/2]}{\Gamma[(n/2)+1]}\right\}^2.$$

Solutions for intermediate values of $\bar{\tau}$ can be easily found from (24) by trial and error. In the upper half of Fig. 2 values of λ_c, normalized by λ_0, are plotted for the allowable range of $\bar{\tau}$ for the cases $n = 1$, 2 and 3.

Initial postbuckling solution

All of the information needed to determine the initial postbuckling behavior of minimum-gage-constrained optimal columns has already been listed. Substitution of the solutions (20)–(24) into (16) and (17) allows H to be determined. This calculation is rather lengthy, but simple, and leads to the result

$$H = \frac{n}{[(n+1)\hat{\tau}-n]^2}\left[\frac{n+1}{n+4}\right]\left\{4\xi_0\bar{\tau}(\bar{\tau}-\hat{\tau}) + \frac{n-2}{2}\bar{\tau}\left[\frac{n+2}{n+1}-\hat{\tau}\right]+\frac{\hat{\tau}}{2}\left[\frac{(n+1)(n+4)}{n}\hat{\tau}-(n+6)\right]\right\}. \tag{25}$$

Values of H for the limiting cases of $\bar{\tau} = 0$ and $\bar{\tau} = 1$ are easily found from (25). Recall that when $\bar{\tau} = 1$, (the prismatic column), $\hat{\tau} = 1$ and $\xi_0 = \frac{1}{2}$, so $H = \frac{1}{2}$ for all n. Also, when $\bar{\tau} = 0$, (the unconstrained optimal column) $\hat{\tau} = (n+2)/(n+1)$ and $\xi_0 = 0$, so, $H = (n+2)/(n+4)$. Values of H corresponding to intermediate values of $\bar{\tau}$ can be easily found from (25) knowing the gage-constrained optimal solutions. In the lower half of Fig. 2, values of H are plotted against the same abscissa as in the upper half of the figure, also for the cases $n = 1$, 2 and 3.

It is interesting to note that the optimized columns have greater initial postbuckling stiffness than the prismatic columns. This is however of little consequence. In all cases the initial postbuckling stiffnesses are numerically so small that they are in fact insignificant.

CIRCULAR PLATES

Prebuckling, buckling and initial postbuckling equations

The equations for the analysis of flat, simply-supported, axisymmetric circular plates, loaded by radial thrust are now reproduced [8]. These equations are more complicated than those for the columns just considered. This is in part a consequence of the fact that the plates are statically indeterminate, hence the prebuckling stress field must be calculated.

The bending and stretching force equilibrium equations for the axisymmetric deformation of a circular plate, subject only to in-plane loading, are

$$\frac{\mathrm{d}}{\mathrm{d}r}(rM_r)-M_t+rN_r\frac{\mathrm{d}W}{\mathrm{d}r}=0 \tag{26}$$

$$\frac{\mathrm{d}}{\mathrm{d}r}(rN_r)-N_t=0 \tag{27}$$

where M_r, M_t, N_r and N_t are the radial and tangential moments and forces and W is the out-of-plane displacement, as shown in Fig. 3. If a stress function Φ is defined by

$$N_r = \frac{\Phi}{r}, \qquad N_t = \frac{\mathrm{d}\Phi}{\mathrm{d}r} \tag{28}$$

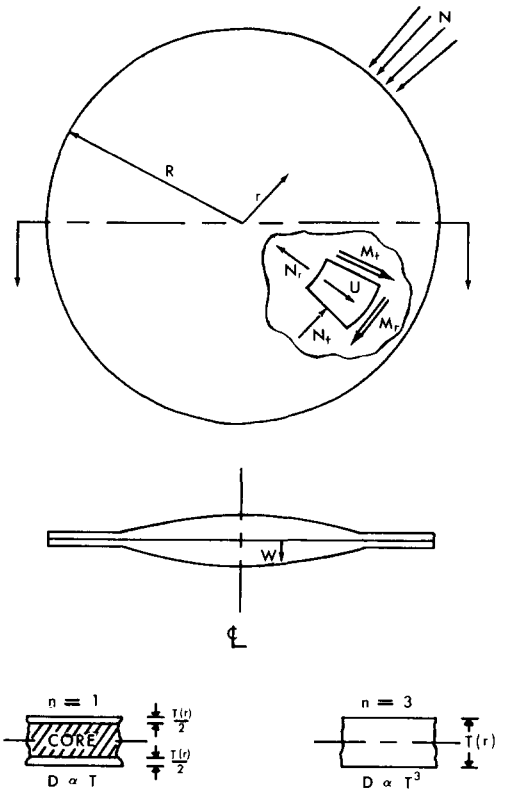

FIG. 3. Circular plate geometry, displacements, forces and moments.

it serves to satisfy (27) identically. The force–distortion and moment–distortion relations for an axisymmetric plate are

$$N_r = \frac{ET(r)}{1-v^2}\left[\frac{dU}{dr} + \frac{v}{r}U + \frac{1}{2}\left(\frac{dW}{dr}\right)^2\right]$$
$$N_t = \frac{ET(r)}{1-v^2}\left[\frac{U}{r} + v\frac{dU}{dr} + \frac{v}{2}\left(\frac{dW}{dr}\right)^2\right] \tag{29}$$

$$M_r = -D(r)\left[\frac{d^2W}{dr^2} + \frac{v}{r}\frac{dW}{dr}\right]$$
$$M_t = -D(r)\left[\frac{1}{r}\frac{dW}{dr} + v\frac{d^2W}{dr^2}\right] \tag{30}$$

where E is Young's modulus, v Poisson's ratio, T the effective thickness of structural material, U the radial displacement and D the plate bending stiffness.

As with the column problem, it is convenient for our purposes to relate the plate bending stiffness to the thickness of the structural material. For the class of plates under consideration

$$D(r) = kEV\left[\frac{\pi R^2 T(r)}{V}\right]^n \tag{31}$$

where k and n are arbitrary, positive constants, R the plate radius and V the total volume of structural material:

$$2\pi \int_0^R T(r) r \, \mathrm{d}r = V. \tag{32}$$

With appropriate choices of k, the cases $n = 1$ and $n = 3$ model, respectively, sandwich plates with a light core of uniform thickness and face-sheets of variable thickness, and solid plates of variable thickness (see Fig. 3).

Equations (26) and (28)–(31) can be readily combined to give the compatibility and equilibrium relations of plate theory. These are, respectively, in non-dimensional form

$$\left[\frac{1}{\tau}(\xi\phi' - \nu\phi)\right]' + \frac{1}{\tau}\left(\nu\phi' - \frac{\phi}{\xi}\right) - \eta^2 = 0 \tag{33}$$

$$[\tau^n(\xi\eta' + \nu\eta)]' - \tau^n\left(\nu\eta' + \frac{\eta}{\xi}\right) + \phi\eta = 0 \tag{34}$$

where

$$\tau = \frac{\pi R^2 T}{V}, \qquad \phi = -\frac{R\Phi}{kEV}, \qquad \eta = \frac{1}{(2\pi k)^{\frac{1}{2}}}\frac{\mathrm{d}W}{\mathrm{d}r}, \qquad \xi = \frac{r}{R} \quad \text{and} \quad (\,)' = \frac{\mathrm{d}}{\mathrm{d}\xi}(\,).$$

(Note that the minus sign is included in the definition of ϕ so that it is positive for compressive radial stress.) The appropriate boundary conditions for a simply-supported plate, with an applied compressive radial force/unit circumferential length, N, as shown in Fig. 3, are

$$\begin{aligned} \phi &= 0 \quad \text{at} \quad \xi = 0 \\ \phi &= \lambda \quad \text{at} \quad \xi = 1 \end{aligned} \tag{35}$$

$$\begin{aligned} \eta &= 0 \quad \text{at} \quad \xi = 0 \\ \tau^n(\xi\eta' - \nu\eta) &= 0 \quad \text{at} \quad \xi = 1 \end{aligned} \tag{36}$$

where $\lambda = R^2 N/kEV$ is the non-dimensional loading factor.

In reference [6] Budiansky provides a compendium of formulas for analyzing postbuckling behavior within the context of Donnell–Mushtari–Vlasov shell theory. These formulas are easily modified to be consistent with the present formulation. A perturbation solution is sought near the bifurcation point in the form

$$\begin{Bmatrix} \phi \\ \eta \end{Bmatrix} = \lambda \begin{Bmatrix} \phi_0 \\ 0 \end{Bmatrix} + \varepsilon \begin{Bmatrix} \phi_1 \\ \eta_1 \end{Bmatrix} + \varepsilon^2 \begin{Bmatrix} \phi_2 \\ \eta_2 \end{Bmatrix} + \ldots \tag{37}$$

$$\lambda = \lambda_c[1 + a\varepsilon + b\varepsilon^2 + \ldots] \tag{38}$$

where it is seen that $\lambda \to \lambda_c$ as $\varepsilon \to 0$. Note that it is already assumed in (37) that no out-of-plane displacement occurs prior to buckling. If (37) and (38) are substituted into (33)–(36), and the resulting equations are linearized with respect to ε, the desired set of equations results. These equations are:

$$\left[\frac{1}{\tau}(\xi\phi_0' - \nu\phi_0)\right]' + \frac{1}{\tau}\left(\nu\phi_0' - \frac{\phi_0}{\xi}\right) = 0$$
$$\phi_0 = 0 \quad \text{at } \xi = 0, \qquad \phi_0 = 1 \quad \text{at } \xi = 1 \tag{39}$$

$$[\tau^n(\xi\eta_1' + \nu\eta_1)]' - \tau^n\left(\nu\eta_1' + \frac{\eta_1}{\xi}\right) + \lambda_c\phi_0\eta_1 = 0$$
$$\eta_1 = 0 \quad \text{at } \xi = 0, \qquad \tau^n(\xi\eta_1' + \nu\eta_1) = 0 \quad \text{at } \xi = 1 \tag{40}$$

$$\left[\frac{1}{\tau}(\xi\phi_2' - \nu\phi_2)\right]' + \frac{1}{\tau}\left(\nu\phi_2' - \frac{\phi_2}{\xi}\right) = \eta_1^2$$
$$\phi_2 = 0 \quad \text{at } \xi = 0, \qquad \phi_2 = 0 \quad \text{at } \xi = 1. \tag{41}$$

It is readily concluded from the form of the governing equations that $\phi_1 \equiv 0$ and $\eta_2 \equiv 0$, hence these equations are not listed.

The buckling mode is normalized by fixing the value of the deflection of the center of the plate. This is done by choosing

$$\int_0^1 \eta_1 \, d\xi = 1. \tag{42}$$

This allows ε to be interpreted as a measure of the contribution of the buckling mode η_1 to the buckled state. Also, the higher order terms in the expansion of η are required to be orthogonal to η_1 by the relation

$$\int_0^1 \phi_0\eta_1\eta_j \, d\xi = 0 \quad \text{for } j = 2, 3, \ldots \tag{43}$$

With these definitions made, the equations needed to analyze the postbuckling behavior of circular plates can be readily obtained from [6] in the form:

$$\lambda_c = \frac{\int_0^1 \tau^n\{[\eta_1' + (\nu/\xi)\eta_1]^2 + (1-\nu^2)(\eta_1/\xi)^2\}\xi \, d\xi}{\int_0^1 \phi_0\eta_1^2 \, d\xi} \tag{44}$$

$$a = 0 \tag{45}$$

$$b = -\frac{\int_0^1 \phi_2\eta_1^2 \, d\xi}{\lambda_c\int_0^1 \phi_0\eta_1^2 \, d\xi}. \tag{46}$$

Once again it is found that $a = 0$, hence the initial postbuckling behavior depends upon the magnitude and sign of b. If (41) is used to eliminate η_1 from the numerator integral in (46) and one integration by parts performed, it is readily concluded from the resulting equation that $b > 0$. Therefore, all the plates are insensitive to initial imperfections.

As with the column problems, the magnitude of b depends upon the normalization of the buckling mode. Instead of using b as a measure of the initial postbuckling behavior, it seems wise to choose the ratio K of the postbuckling to prebuckling stiffness of the

plate, as this quantity is independent of the normalization of η_1. (Note that K for the plate problems has a different interpretation than H for the column problems.) An expression for K can be found in [6] in the form

$$K = \left[1 + \frac{\int_0^1 \phi_0 \eta_1^2 \, d\xi}{b\lambda_c\{(\xi\phi_0/\tau)[\phi_0' - (v/\xi)\phi_0]\}_{\xi=1}}\right]^{-1}. \tag{47}$$

This relates the load to the generalized deflection through the relation

$$\left(\frac{\lambda}{\lambda_c} - 1\right) = K\left(\frac{\Delta}{\Delta_c} - 1\right) \tag{48}$$

where $\lambda\Delta$ is the decrease in the potential energy of the loads. (The significance of K is shown by the insert in Fig. 4.) Since $b > 0$, it is expected that the range of K for the plates is $0 < K < 1$. Also, the larger the value of K, the smaller the reduction of stiffness immediately after buckling.

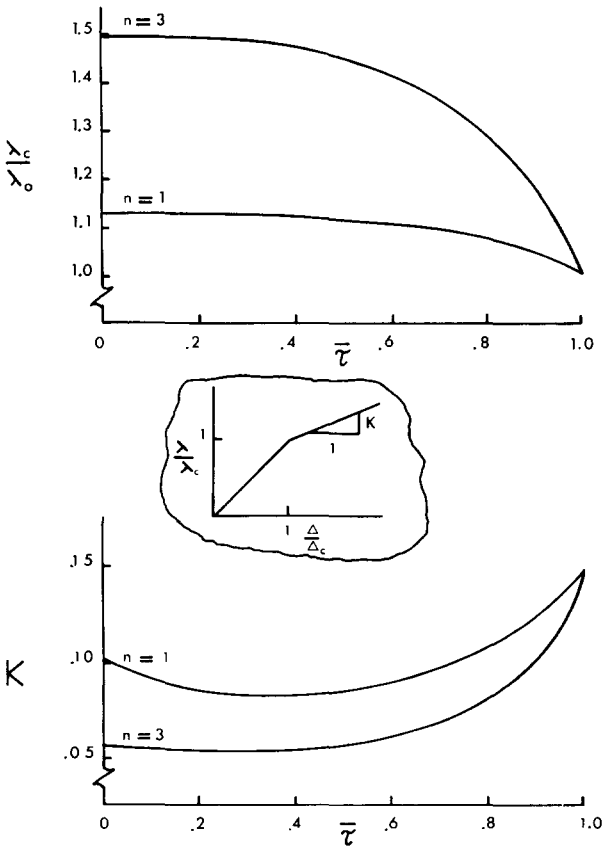

FIG. 4. Buckling and initial postbuckling behavior of circular plates.

Constrained optimal design equations and solution

Optimization is achieved by choosing the thickness of structural material so as to maximize the buckling load λ_c (44) while maintaining the volume of structural material fixed. The volume restriction is given by (32), which in terms of the non-dimensional variables assumes the form

$$\int_0^1 \tau(\xi)\xi \, d\xi = \tfrac{1}{2}. \tag{49}$$

The additional restriction is imposed that the thickness of the structural material may not fall below a specified value, $\bar{T}$. In non-dimensional form, this requires that

$$\tau \geq \bar{\tau} \tag{50}$$

where $\bar{\tau} = \pi R^2 \bar{T}/V$. It is well known that the sum of the principal stresses is constant in regions of uniform plate thickness. Therefore, the thickness constraint could be interpreted as being a limitation on the maximum allowable average prebuckling stress.

Two regions of solution are identified; ones where the constraint is active ($\tau = \bar{\tau}$), and ones where it is inactive ($\tau > \bar{\tau}$). By analogy to the column solutions, the constraint is only active in an annular region extending from the simply-supported edge of the plate inward to some point which is determined during the solution by the value of $\bar{\tau}$. Comparison of (49) and (50) leads to the conclusion that $\bar{\tau} \leq 1$. Also, since on physical grounds thickness cannot be negative, the allowable range of $\bar{\tau}$ is $0 \leq \bar{\tau} \leq 1$.

Since the problem being discussed is solved in [8], no further details are included here. It is noted that the complexity of the governing equations inspires a numerical solution. The character of the results is identical to that for the gage constrained optimal columns. The limiting case of $\bar{\tau} = 1$ is the well-known prismatic plate, for which the classical buckling eigenvalue is given by $\lambda_c \equiv \lambda_0 = 4{\cdot}197$ when $\nu = 0{\cdot}3$. In the upper half of Fig. 4, values of the classical buckling load λ_c, normalized by λ_0, are plotted for the allowable range of $\bar{\tau}$ for $\nu = 0{\cdot}3$ and $n = 1$ and 3.

Initial postbuckling solution

Once the constrained optimal plate geometries are known, the postbuckling behavior is easily determined. The solutions to (39)–(41) are substituted into (46) and (47) to determine the postbuckling to prebuckling stiffness ratio K. In the lower half of Fig. 4, values of K are shown for the allowable range of $\bar{\tau}$, for $\nu = 0{\cdot}3$ and $n = 1$ and 3. Notice by comparing the upper and lower halves of Fig. 4 that as the buckling loads increase as a consequence of relaxing the level of the thickness constraint, the value of K first decreases and then increases. For both cases investigated the initial postbuckling stiffness for the uniform thickness plate is larger than for any of the optimized plates. It is also interesting to note that the smallest value of K in each case occurs for intermediate levels of the thickness constraint.

CONCLUDING REMARKS

The initial postbuckling behavior of constrained, optimally designed columns and circular plates was investigated. For the columns the slope immediately after buckling of the load vs. end shortening curve was used as a measure of the postbuckling behavior. This

quantity was found to increase a little along with increases in the buckling load when the gage constraint was relaxed. The numerical values found for the slope of the load vs. end shortening curve are however so small that the increase observed is really inconsequential.

For the plates, the ratio of the postbuckling to prebuckling stiffness was chosen as a measure of the initial postbuckling behavior. It was found that the uniform thickness plate exhibits a larger value of this quantity than any of the optimized plates. In addition there was an intermediate range of values of the thickness constraint which had associated smaller values of the initial postbuckling stiffness than were found for the unconstrained optimal plates.

REFERENCES

[1] B. BUDIANSKY and J. W. HUTCHINSON, A survey of some buckling problems. *AIAA Jl* **4**, 1505–1510 (1966).
[2] J. W. HUTCHINSON and J. C. AMAZIGO, Imperfection-sensitivity of eccentrically stiffened cylindrical shells. *AIAA Jl* **5**, 392–401 (1967).
[3] E. F. MASUR, Buckling, postbuckling and limit analysis of completely symmetric elastic structures. *Int. J. of Solids Struct.* **6**, 587–604 (1970).
[4] W. T. KOITER, On the stability of elastic equilibrium, (in Dutch), Thesis, Delft, Amsterdam (1945); English translation issued as NASA TT F-10, 833 (1967).
[5] B. BUDIANSKY, Dynamic buckling of elastic structures: criteria and estimates, *Proc. Int. Conf. on Dynamic Stability of Structures*, Evanston, Illinois. Pergamon Press (1965).
[6] B. BUDIANSKY, Postbuckling behavior of cylinders in torsion, *Proc. Second IUTAM Symp. on the Theory of Thin Shells*, Copenhagen, edited by F. I. NIORDSON, Springer (1969).
[7] J. C. FRAUENTHAL, Constrained optimal design of columns against buckling, Report SM-49, DEAP, Harvard University, Cambridge, Massachusetts (1971). *J. struct. Mech.* to be published.
[8] J. C. FRAUENTHAL, Constrained optimal design of circular plates against buckling, Report SM-50, DEAP, Harvard University, Cambridge, Massachusetts (1971). *J. struct. Mech.* to be published.
[9] W. PRAGER and J. E. TAYLOR, Problems of optimal structural design. *J. appl. Mech.* **35**, 102–106 (1968).
[10] J. B. KELLER, The shape of the strongest column. *Archs ration. Mech. Analysis* **5**, 275–285 (1960).
[11] B. BUDIANSKY, J. C. FRAUENTHAL and J. W. HUTCHINSON, On optimal arches. *J. appl. Mech.* **36**, 880–882 (1969).

(*Received* 3 *March* 1972; *revised* 24 *April* 1972)

Абстракт—Исследуется начальное поведение двух общих типов конструкций, проектированных на минимум веса. Эти конструкции представляют собой прямые, свободно опертые колонны, нагруженные осебым давлением, или плоские, свободно опертые, осесимметрические круглые пластинки, нагруженные радиальным давлением. Смысл расчета конструкций на оптимум веса такой, что они могут выдерживать найбольшую из возможных нагрузок, удовлетворя заданному обьему и минимуму допускаемой меры сил связы. Анализ устойчивости основан на общей теории Койтера поведения конструкций после выпучивания.